Electronic Supplementary Material

"Charging" the cigarette butt: heteroatomic porous carbon nanosheets with edge-induced topological defects for enhanced oxygen evolution performance

Qing-Hui Kong[1], Xian-Wei Lv[1], Jin-Tao Ren[1], Hao-Yu Wang[1], Xin-Lian Song[1], Feng Xu (✉)[2], Zhong-Yong Yuan (✉)[2,3]

1 School of Materials Science and Engineering, Smart Sensing Interdisciplinary Science Center, Nankai University, Tianjin 300350, China

2 Tianjin Workstation, Technology Center of Shanghai Tobacco Group Co. Ltd., Tianjin 300163, China

3 Key Laboratory of Advanced Energy Materials Chemistry (Ministry of Education), Nankai University, Tianjin 300071, China

E-mails: zyyuan@nankai.edu.cn; xfrong99@sina.com (Xu F)

1. Supplementary Experimental

1.1. Chemicals and materials

Cobalt chloride hexahydrate ($CoCl_2·6H_2O$), iron trichloride hexahydrate ($FeCl_3·6H_2O$), urea and potassium hydroxide were purchased from Tianjin Bohua Technology Co., Ltd. Nickel chloride hexahydrate ($NiCl_2·6H_2O$) was purchased from Shanghai Xushuo biotechnology Co., Ltd. The powder of cobalt was purchased from Shanghai Macklin Biochemical Co., Ltd. Cigarette butts were collected from common areas in Tianjin.

1.2. Characterization

X-ray diffraction (XRD) patterns were obtained on a Bruker D8 Focus diffractometer with Cu−*K*α radiation (λ = 0.15418 nm) operated at 40 kV and 40 mA. X-ray photoelectron spectroscopy (XPS) was performed on the ESCALAB 250Xi. The morphology of the samples was taken on JEOL JSM-7800F scanning electron microscope (SEM) and JEOL JEM-2800 transmission electron

microscopy (TEM). Specific surface area and pore volume of samples were analyzed by the multi-point Brunauer–Emmett–Teller (BET) method. The pore size distribution curve was obtained from the adsorption branch according to the density functional theory (DFT) method. And total pore volume was determined from the volume adsorbed at the relative pressure (P/P_0) of 0.99.

1.3. Electrochemical measurement

The electrochemical experiments were conducted on a WaveDriver 20 Bipotentiostat/Galvanostat (Pine Research Instrumentation, USA) workstation using a standard three-electrode system. The Ag/AgCl and platinum wire were used as the reference and counter electrode, respectively. For the preparation of the working electrode, 5.0 mg catalyst was ultrasonically dispersed in the mixed solution containing 95 μL of isopropanol, 385 μL of deionized water, and 20 μL of Nafion (5 wt%) solution to obtain the homogeneous catalyst suspension. Then, the prepared carbon-paper (1 × 1 cm^2) loaded with catalyst were used as the working electrode for OER and ORR electrochemical testing, and the loading mass is 1.0 mg cm^{-2}. Linear sweeping voltammetry (LSV) polarization curves for OER and ORR were conducted in 1.0 M KOH solution All potentials were calibrated to the reversible hydrogen electrode (RHE) based on the equation:

$$E_{\text{vs RHE}} = E_{\text{vs Ag/AgCl}} + 0.059 \times \text{pH} + E^{o}_{\text{Ag/AgCl}}.$$

1.4. Zn−Air Battery Measurements.

The aqueous Zn-air battery was fabricated by using Zn plate as the anode and the catalyst ink-coated carbon paper (the loading mass of 1.0 mg cm^{-2}) as the air cathode. The electrolyte of the aqueous Zn−air battery was 6.0 M KOH and 0.2 M $Zn(Ac)_2$ solution. The solid state Zn−air battery was fabricated by the catalyst ink-coated carbon cloth as flexible cathode, Zn foil as the anode and alkaline polyvinyl alcohol (PVA) as the gel electrolyte. The PVA (2.0 g) powder was dissolved in 20 mL of deionized water with stirring at 95 ℃, and 6.0 mL of the mixture of 6.0 M KOH and 0.2 M $Zn(Ac)_2$ was added into the above solution. The gel was frozen and thawed at room temperature. The charging-discharging polarization curves were conducted on a Zahner IM6eX workstation and the long-term cycling measurements of assembled rechargeable ZABs were executed on LAND CT2001A instrument.

2. Supplementary Figures

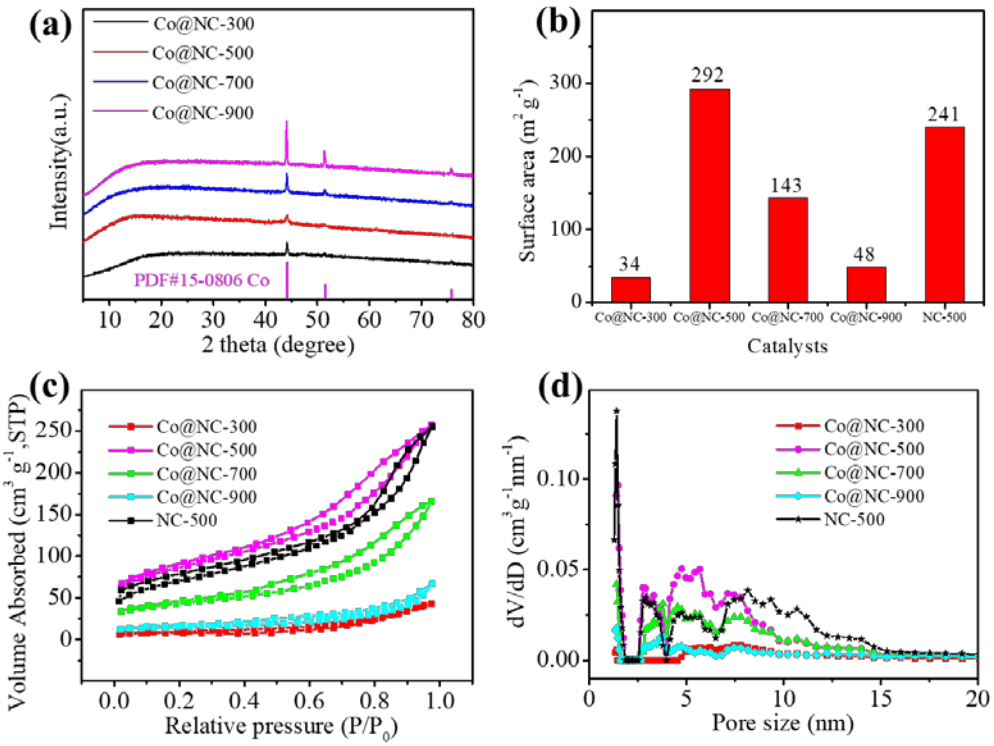

Figure S1. (a) XRD pattern of Co@NC-*T*. (b) Surface area, (c) N_2 adsorption-desorption isotherms and (d) corresponding pore size distributions of Co@NC-*T* and NC-500.

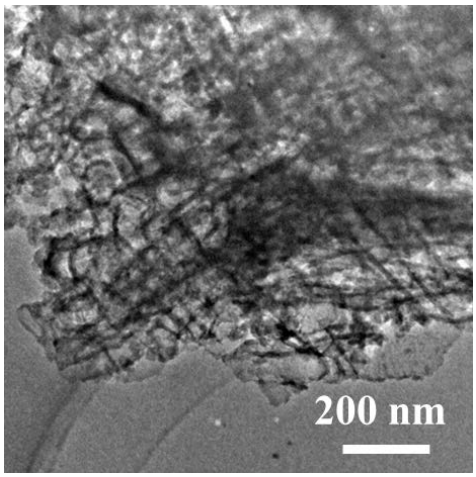

Figure S2. TEM image of NC-500

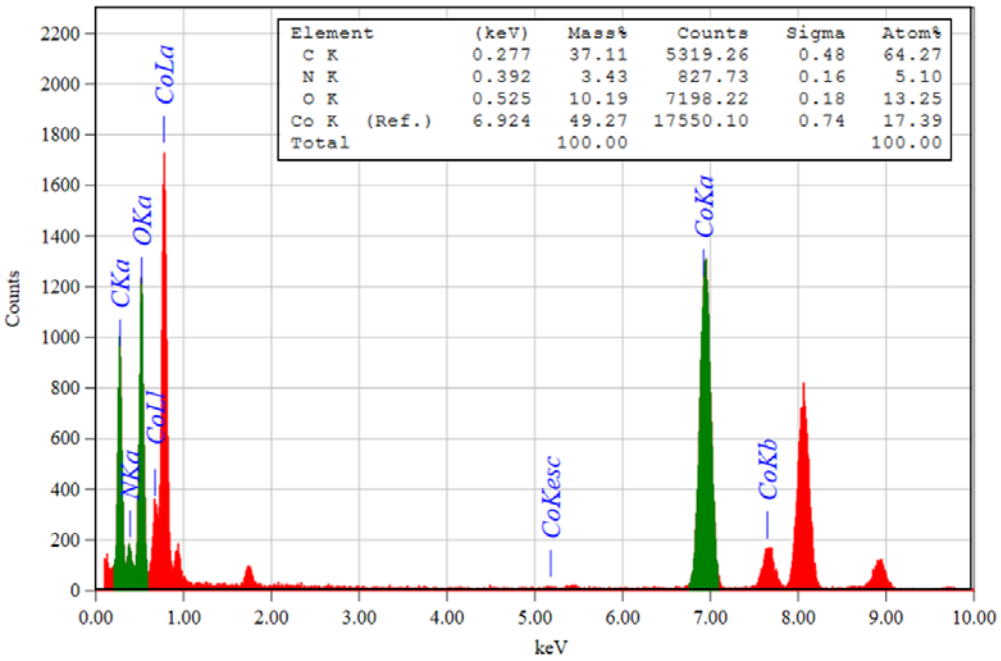

Figure S3. EDX spectrum of the obtained Co@ NC-500.

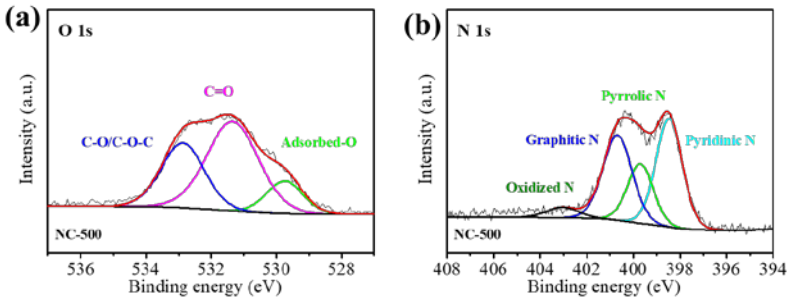

Figure S4. The high-resolution XPS spectra (a) O 1s and (b) N 1s of NC-500.

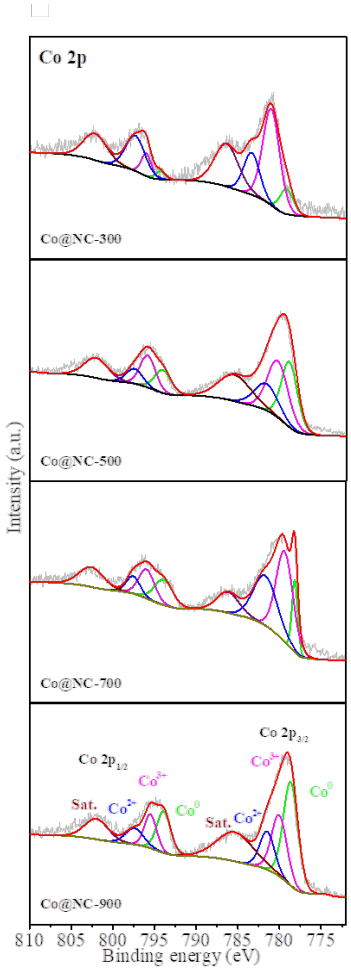

Figure S5. The high-resolution XPS spectra Co 2p of Co@NC-*T*.

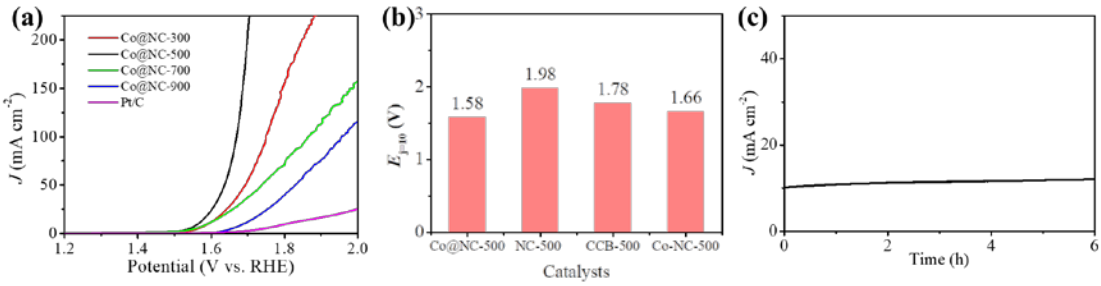

Figure S6. (a) OER polarization curves of the catalysts in 1.0 M KOH. (b) The $E_{j=10}$ of the as-prepared catalysts. (c) Chronoamperometric responses of Co@NC-500 at 1.58 V.

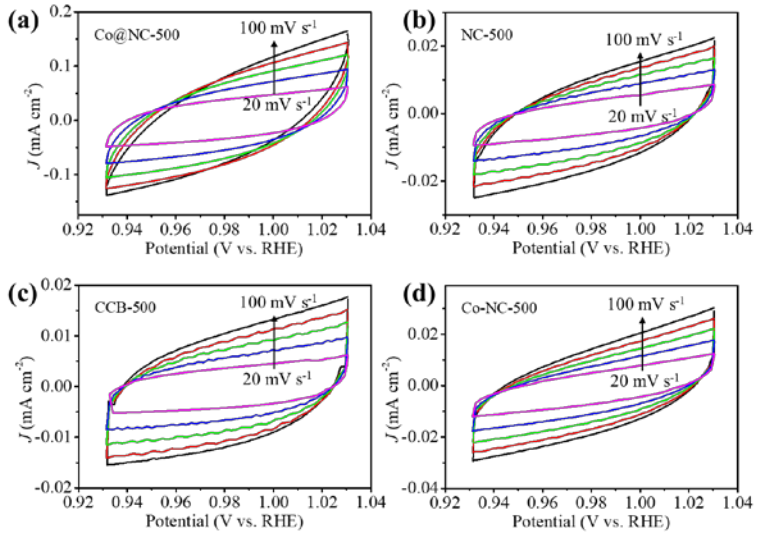

Figure S7. Cyclic voltammograms of the as-prepared catalysts measured at different scan rates ranging from 20 to 100 mV s^{-1}.

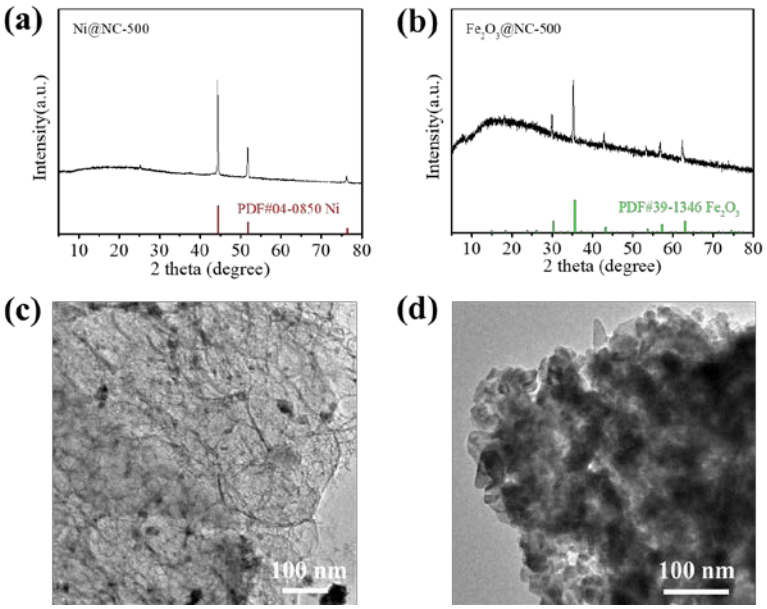

Figure S8. (a, b) XRD pattern of Ni@NC-500 and Fe_2O_3@NC-500. (c, d) TEM images of Ni@NC-500 and Fe_2O_3@NC-500.

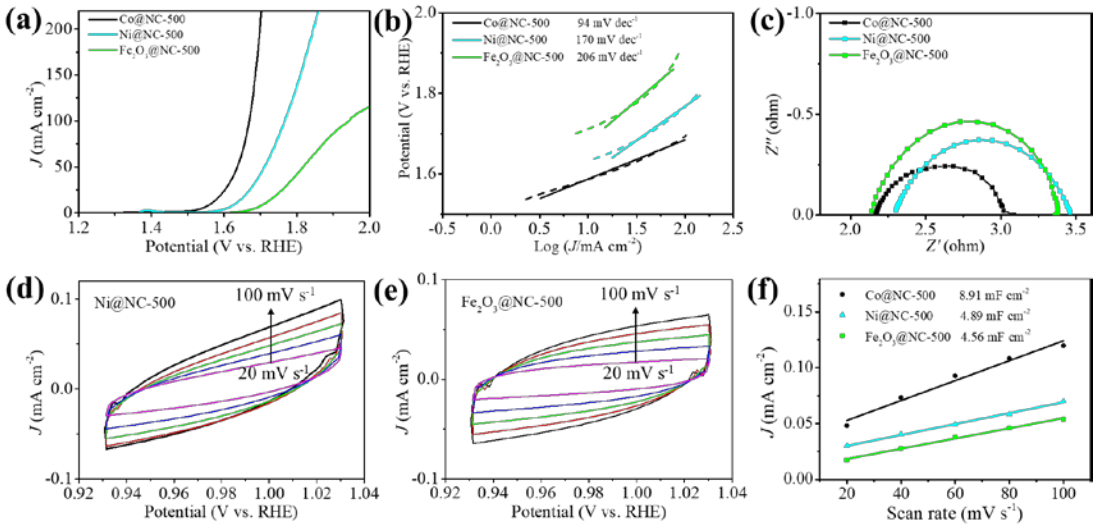

Figure S9. (a) OER polarization curves of the catalysts in 1.0 M KOH. (b) Tafel plots and (c) EIS of the as-prepared catalysts. (d, e) Cyclic voltammograms of the as-prepared catalysts measured at different scan rates ranging from 20 to 100 mV s^{-1}. (f) Electrochemical double-layer capacitance of the catalysts.

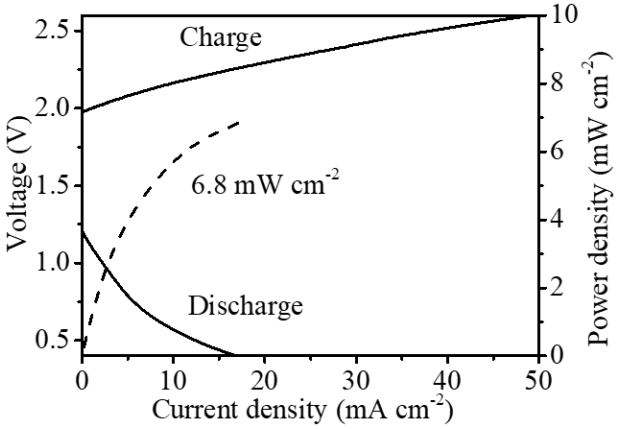

Figure S10. Charge−discharge performance and corresponding power densities assembled with Co@NC-500 catalyst of rechargeable solid Zn−air batteries.

3. Supplementary Tables

Table S1. Comparison of OER activities between Co@NC-500 and some recently reported catalysts.

Catalyst	Carbon precursor	$E_{j=10}$ (V vs. RHE)	Ref.
Co@NC-500	cigarette butts	1.58	This work.
FeCo@NS-CA	wood	1.68	[1]
FeNi-NC	peanut shells	1.64	[2]
FeNi@NCNT-CP	cotton pad	1.59	[3]
Co-N/PDC.	peat	1.59	[4]
NPCSS	corn stalk	1.59	[5]
PAN-CCC	cotton cloth	1.58	[6]
CoZn-NC-700	ZIFs	1.62	[7]
CoS_x@Cu_2MoS_4-MoS_2/NSG	graphene oxide	1.58	[8]
NB-CN	chitosan	1.62	[9]

References

1. Pang H, Sun P, Gong H, Zhang N, Cao J, Zhang R, Luo M, Li Y, Sun G, Li Y, et al. Wood-derived bimetallic and heteroatomic hierarchically porous carbon aerogel for rechargeable flow Zn-air batteries. ACS Applied Materials & Interfaces, 2021, 13(33): 39458-39469.

2. Yang L, Zeng X, Wang D, Cao D. Biomass-derived FeNi alloy and nitrogen-codoped porous carbons as highly efficient oxygen reduction and evolution bifunctional electrocatalysts for rechargeable Zn-air battery. Energy Storage Materials, 2018, 12: 277-283.

3. Zheng X, Cao X, Zeng K, Yan J, Sun Z, Rummeli M H, Yang R. A self-jet vapor-phase growth of 3D FeNi@NCNT clusters as efficient oxygen electrocatalysts for zinc-air batteries. Small, 2021, 17(4): e2006183.

4. Teppor P, Jäger R, Paalo M, Palm R, Volobujeva O, Härk E, Kochovski Z, Romann T, Härmas R, Aruväli J, et al. Peat-derived carbon-based non-platinum group metal type catalyst for oxygen reduction and evolution reactions. Electrochemistry Communications, 2020, 113: 106700.

5. Liu Z, Zhou Q, Zhao B, Li S, Xiong Y, Xu W. Few-layer N-doped porous carbon nanosheets derived from corn stalks as a bifunctional electrocatalyst for overall water splitting. Fuel, 2020, 280: 118567.

6. Zhang C, Bhoyate S, Hyatt M, Neria B L, Siam K, Kahol P K, Ghimire M, Mishra S R, Perez F, Gupta R K. Nitrogen-doped flexible carbon cloth for durable metal free electrocatalyst for overall water splitting. Surface and Coatings Technology, 2018, 347: 407-413.

7. Chen B, He X, Yin F, Wang H, Liu D-J, Shi R, Chen J, Yin H. MO-Co@N-doped carbon (M = Zn or Co): vital roles of inactive Zn and highly efficient activity toward oxygen reduction/evolution

reactions for rechargeable Zn-air battery. Advanced Functional Materials, 2017, 27(37): 1700795.
8. Nguyen D C, Tran D T, Doan T L L, Kim D H, Kim N H, Lee J H. Rational design of core@shell structured CoSx@Cu_2MoS_4 hybridized MoS2/N,S-codoped graphene as advanced electrocatalyst for water splitting and Zn-air battery. Advanced Energy Materials, 2020, 10(8): 1903289.
9. Lu Z, Wang J, Huang S, Hou Y, Li Y, Zhao Y, Mu S, Zhang J, Zhao Y. N,B-codoped defect-rich graphitic carbon nanocages as high performance multifunctional electrocatalysts. Nano Energy, 2017, 42: 334-340.